Inorg. Chem. **2005**, *44*, 5996–6003

Ruthenium(II) Complexes of 1,12-Diazaperylene and Their Interactions with DNA

Abdellatif Chouai,[†] Sara E. Wicke,[‡] Claudia Turro,*[,‡] John Bacsa,[§] Kim R. Dunbar,[§] Dong Wang,[†] and Randolph P. Thummel*[,†]

Department of Chemistry, University of Houston, Houston, Texas 77204-5003, Department of Chemistry, The Ohio State University, Columbus, Ohio 43210-1185, and Department of Chemistry, Texas A&M University, P.O. Box 30012, College Station, Texas 77842-3012

Received October 7, 2004

Four complexes of the ligand 1,12-diazaperylene (DAP) have been prepared, $[Ru(bpy)_n(DAP)_{3-n}]^{2+}$ where $n =$ 0–2 and $[Ru(DAP)_3]^{2+}$. The $[Ru(DAP)_3]^{2+}$ complex was characterized by X-ray analysis and was found to exhibit the expected propeller-like structure with significant intermolecular π-stacking interactions. The three Ru(II) complexes showed self-consistent optoelectronic properties with similar ligand-centered $\pi-\pi^*$ absorptions in the range of 333–468 nm and MLCT bands associated with the DAP which increased in intensity and decreased in energy as the number of DAP ligands varied from 1 to 3. Hypochromicity and viscosity changes were observed that were consistent with DAP intercalation into DNA, and binding constants were measured in the range of $1.4–1.6 \times 10^6$ M^{-1} for the mixed ligand complexes. Furthermore, the complex $[Ru(bpy)_2(DAP)]^{2+}$ was found to photocleave plasmid DNA upon irradiation with visible light.

Introduction

The complexes of Ru(II) with 2,2′-bipyridine (bpy) are one of the most widely studied of all coordination compounds.[1] One source of this interest is the potential of the photoexcited state of a complex such as $[Ru(bpy)_3]^{2+}$ to act as an effective redox catalyst. Oxidation and reduction processes mediated by this excited state are driven by the energy of the light absorbed by the complex, leading to a wide range of photochemically attractive applications. The energy of the absorbed light thus, to some extent, dictates the subsequent photochemistry that may occur.

The lowest-energy excited state of a Ru(II) polypyridine complex corresponds to the longest wavelength electronic absorption and is generally associated with a metal-to-ligand charge transfer (MLCT) excited state.[2] This state involves the promotion of an electron from a d-orbital of Ru(II) to the π^*-level of one of the ligands. Thus, the nature of the ligands exerts a profound influence on the absorption properties of the complex. Ligands that bear electronegative substituents or those with delocalized π-systems are better electron acceptors, have lower energy π^*-levels, and give rise to longer wavelength absorptions. An unfortunate consequence of lowering the π^*-energy level by too great an extent, however, is that other low-lying states begin to compete for depopulation of the singlet MLCT state such that the excited state lifetime is drastically reduced, and the complex becomes nonemissive.

Given the considerable importance of 1,10-phenanthroline (**1**, phen) as an analogue to bpy, we became interested in the methodical modification of this ligand to increase π-delocalization while retaining the C_2-symmetry.[3] This modification may be accomplished by judicious benzo fusion, leading to the benzo- and naphtho-fused phens **2** and **3** as well as the dibenzo-fused **4**.

Diazatriphenylene (**2**) is prepared by a double Skraup reaction on 2,3-diaminonaphthalene.[4] Its complexation with

* To whom correspondance should be addressed. E-mail: thummel@uh.edu (R.P.T.), turro.1@osu.edu (C.T.).
[†] University of Houston.
[‡] The Ohio State University.
[§] Texas A&M University.

(1) (a) Kalyanasundaram, K. *Photochemistry of Polypyridine and Porphyrin Complexes*; Academic Press: San Diego, 1992. (b) Juris, A.; Balzani, V.; Barigelletti, F.; Campagna, S.; Belser, P.; von Zelewsky, A. *Coord. Chem. Rev.* **1988**, *84*, 85.
(2) Roundhill, D. M. *Photochemistry and Photophysics of Metal Complexes;* Plenum: New York, 1994; p 165.
(3) Thummel, R. P. Recent Advances in the Synthesis and Chemistry of 1,10-Phenanthroline Derivatives. In *Advances in Nitrogen Heterocycles*; Moody, C. J., Ed.; JAI Press: Stamford, NY, 2000; Vol. 4, p 107.
(4) Thang, D. C.; Jacquignon, P.; Dufour, M. *J. Heterocycl. Chem.* **1976**, *13*, 641.

10.1021/ic0485965 CCC: $30.25
Published on Web 07/19/2005

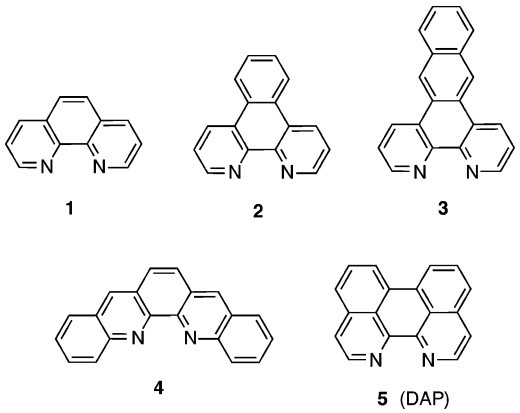

lanthanides has been discussed, but no reports of its complexation with Ru(II) have been published.[5] The naphtho-fused analogue **3** was recently reported by Albano and co-workers.[6] Surprisingly, the mixed ligand complex $[Ru(bpy)_2(\mathbf{3})]^{2+}$ was found to exhibit photophysical properties consistent with a two-component excited state. One component resembles the parent $[Ru(bpy)_3]^{2+}$ moiety, and the other one is associated with the fused anthracene ligand. We have also prepared the dibenzophen **4**.[7] The complex $[Ru(\mathbf{4})_3]^{2+}$ shows an MLCT absorption at 567 nm, but it is essentially nonemissive at room temperature. In the context of ligands **1**−**4**, we became interested in 1,12-diazaperylene (DAP, **5**) as a phen analogue possessing a larger surface area as well as an increased π-delocalization.

In 2001, Mews and co-workers reported a straightforward synthesis of **5** and its complexation with CdSe.[8] Their synthesis involved the potassium-promoted reductive cyclization of the known 1,1′-biisoquinoline (biiq). More recently, Tor and co-workers also reported the synthesis of **5** through a similar cyclization of biiq bound to Ru(II), but they were unable to labilize the complex to obtain the free ligand **5**.[9] Another reason for the interest in **5** is that it is related to the natural product eilatin which has recently been shown to be a useful bridging ligand with nonequivalent binding sites for Ru(II).[10]

Syntheses and Properties

Following the procedure of Mews, we were able to easily prepare useful quantities of **5** from which a series of four

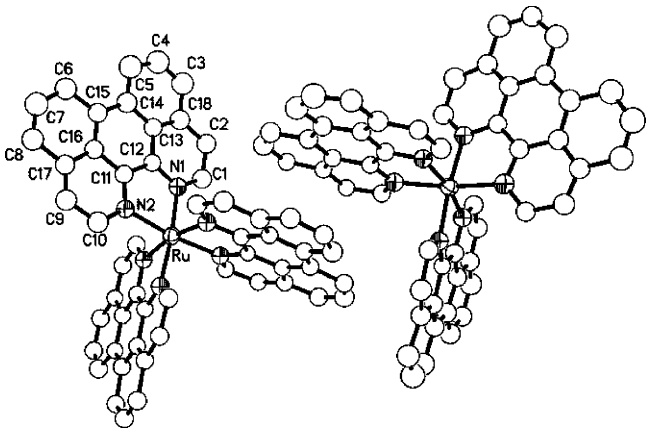

Figure 1. ORTEP plot of the asymmetric unit for the cation of $[Ru(\mathbf{5})_3](PF_6)_2$ showing the atom numbering scheme. Circles take the place of isotropically refined atoms.

Scheme 1

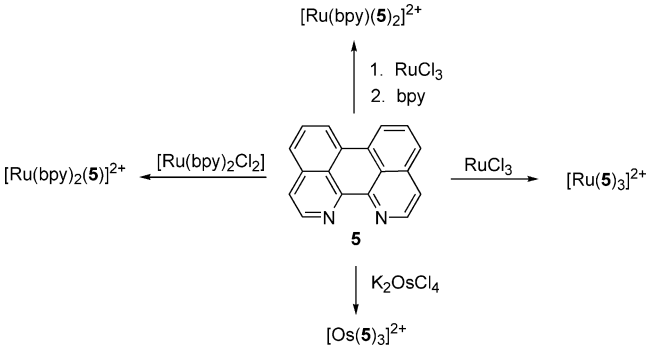

metal complexes were prepared using various combinations of **5** and bpy to complete the coordination sphere of Ru(II) or Os(II). The preparation of these four complexes is outlined in Scheme 1. Each of the complexes possesses at least one symmetry element which is useful for their identification by ^{1}H NMR. An interesting aspect of **5** is that the steric requirements for coordination do not differ significantly from those of the parent phen **1**. Nevertheless, relatively severe conditions (microwave heating in ethylene glycol) were required for complex formation.

A single-crystal X-ray study was carried out on a thin platelet of $[Ru(\mathbf{5})_3](PF_6)_2$. There are 16 formula units in the unit cell, and the asymmetric unit contains 2 $[Ru(DAP)_3]^{2+}$ cations (Figure 1). The $[Ru(DAP)_3]^{2+}$ cations exhibit large distortions from the expected D_{3h}-symmetry, and the pair of $[Ru(DAP)_3]^{2+}$ cations are not related by symmetry, such that each DAP is unique. Because there are two formula units in the asymmetric unit, there are six sets of bond lengths and angles for each DAP. The small crystal size, disorder, and the large unit cell led to weak diffraction. The data-to-parameter ratio was improved by treating the DAP molecules as being related by noncrystallographic symmetry, and the atom labeling scheme for the asymmetric unit is given in Figure 1. DAP may be considered as a dibenzo-fused derivative of 1,10-phenanthroline in which the benzo fusion is at C4−C7, distal from the coordination sites of the ligand. Consequently, the compounds of DAP do not suffer from steric hindrance in the vicinity of metal complexation, and the geometry of $[Ru(DAP)_3]^{2+}$ resembles that of [Ru-

(5) (a) Steemers, F. S.; Verboom, W.; Reinhoudt, D. N.; van der Tol, E. B.; Verhoeven, J. W. *J. Photochem. Photobiol., A* **1998**, *113*, 141−144. (b) Steemers, F. S.; Verboom, W.; Hofstraat, J. W.; Geurts, F. A. J.; Reinhoudt, D. N. *Tetrahedron Lett.* **1998**, *39*, 7583−7586.
(6) (a) Albano, G.; Belser, P.; Daul, C. *Inorg. Chem.* **2001**, *40*, 1408−1413. (b) Albano, G.; Belser, P.; De Cola, L.; Gandolfi, M. T. *Chem. Commun.* **1999**, 1171−1172.
(7) Wu, F.; Thummel, R. P. *Inorg. Chim. Acta* **2002**, *327*, 26−30.
(8) Schmelz, O.; Mews, A.; Basche, T.; Herrmann, A.; Müllen, K. *Langmuir* **2001**, *17*, 2861−2865.
(9) Glazer, E. C.; Tor, Y. *Angew. Chem., Int. Ed.* **2002**, *41*, 4022−4026.
(10) (a) Gut, D.; Rudi, A.; Kopilov, J.; Goldberg, I.; Kol, M. *J. Am. Chem. Soc.* **2002**, *124*, 5449−5456. (b) Bergman, S. D.; Reshef, D.; Frish, L.; Cohen, Y.; Goldberg, I.; Kol, M. *Inorg. Chem.* **2004**, *43*, 3792−3794. (c) Luedtke, N. W.; Hwang, J. S.; Glazer, E.; Gut, D.; Kol, M.; Tor, Y. *ChemBioChem* **2002**, *3*, 766−771. (d) Rudi, A.; Kashman, Y.; Gut, D.; Lellouche, F.; Kol, M. *Chem. Commun.* **1997**, 17−18. (e) Bergman, S. D.; Reshef, D.; Groysman, S.; Goldberg, I.; Kol, M. *Chem. Commun.* **2002**, 2374−2375.

Table 1. Photophysical Data for **5** and Complexes

compound	absorption[a] λ_{max} (nm) (log ϵ)	emission[b] λ_{max} (nm)
5	442(4.37), 417(4.29), 397(3.98), 243(4.47), 201(4.80)	514[a]
$[Ru(\mathbf{5})_3]^{2+}$	588(4.52), 537(4.36), 467(4.65), 441(4.60), 414(4.21), 334(4.50)	727
$[Ru(\mathbf{5})_2(bpy)]^{2+}$	576(4.42), 503(4.15), 468(4.56), 441(4.44), 417(4.19), 334(4.40)	716
$[Ru(\mathbf{5})(bpy)_2]^{2+}$	552(4.22), 467(4.33), 436(4.31), 411(4.00), 333(4.17)	698
$[Os(\mathbf{5})_3]^{2+}$	682(4.04), 621(4.24), 534(3.98), 485(4.17), 459(4.26), 425(4.19), 354(4.28)	763

[a] 10^{-5} M in CH_3CN at 298 K. [b] 10^{-5} M in 4:1 EtOH/MeOH at 77 K, excited at the MLCT wavelength maxima.

$(phen)_3]^{2+}$.[11] The three DAP ligands are approximately planar, with the six inner N-atoms forming a considerably distorted octahedral coordination polyhedron about the central Ru atom. The N−Ru−N angles within the chelate rings are in the range of 77.5(3)−80.0(2)°, whereas the remaining N−Ru−N angles involving different DAP ligands are in the range of 86.7(2)−99.9(2)°. The variable coordination angles are in contrast with those of the first row transition metals which show more regular geometries. Ru(II) ions are designated as being borderline acids on the Pearson scale, have a large number of electrons with many closely spaced energy levels (each with a slightly different electronic configuration), and, therefore, can accommodate a wider variety of coordination environments. The Ru−N bond lengths are normal and are in the range of 2.058(6)−2.105(5) Å, with an average length of 2.08(2) Å and an average N1−Ru−N2 angle of 88(8)°. The dihedral angle between the two coordinating isoquinoline halves of DAP (N2−C11−C12−N1) is only 2(1)°, and the angle between the planes of the complexed DAPs averages 90°. When compared with $[Ru(phen)_3]^{2+}$, the most important structural feature of this complex is the increased π-surface of the DAP ligands, which affords some π-stacking stabilization between the two halves of the asymmetric unit where the distance between the two approximately parallel planes that separate the two DAP molecules is 3.42 Å. This increased π-surface will be important for DNA binding and packing of $[Ru(DAP)_3]^{2+}$ in the crystal and entails optimal π-stacking stabilization of the DAP ligands. This point is illustrated by an expanded view of the unit cell which is included as Supporting Information (Figure S1).

The electronic absorption spectra of the DAP complexes were measured. The data are summarized in Table 1 and illustrated in Figure 2. The free ligand **5** resembles perylene, showing a well-resolved, strong $\pi-\pi^*$ transition at 442 nm. This same transition is evident in the Ru(II) complexes but is shifted by ~25 nm to lower energy. For these three complexes, an MLCT absorbance is observed at longer wavelengths, progressing from 552 to 576 to 588 nm with the successive complexation of additional molecules of **5**. For the Tris complex, the intensity of this band is enhanced and its envelope spans the region of 500−675 nm. At room temperature, the complexes are nonemissive, whereas at 77 K, the three Ru(II) complexes emit weakly in the region of 698−727 nm. For the complex $[Os(\mathbf{5})_3]^{2+}$, the MLCT absorption envelope is even broader and is centered at 682 nm. Interestingly, the $\pi-\pi^*$ component of this absorption is considerably attenuated and less well resolved.

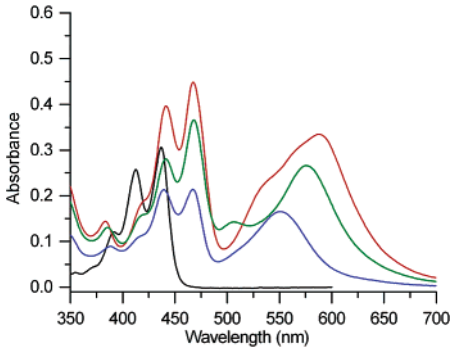

Figure 2. Electronic absorption spectra of **5** (black), $[Ru(\mathbf{5})(bpy)_2]^{2+}$ (blue), $[Ru(\mathbf{5})_2(bpy)]^{2+}$ (green), and $[Ru(\mathbf{5})_3]^{2+}$ (red) in 5×10^{-5} M CH_3CN at 25 °C.

Cyclic voltammetry experiments revealed that the complexes exhibit reversible or quasi-reversible redox couples (Table 2). All three Ru(II) complexes are oxidized at +1.27 V which is very close to the value of +1.29 V observed for $[Ru(bpy)_3]^{2+}$. These oxidations are metal-centered and indicate that the metal d-orbitals are little influenced by complexation with **5** as compared with that of bpy. The reduction processes are ligand-centered and show a nice progression, approaching the free ligand value of −1.26 V, as the number of ligands of **5** around the metal center increases. Reduction of the first bound **5** occurs in the range of −0.59 to −0.71 V. In the case of two molecules of **5** bound to the metal, the second reduction of **5** occurs at −0.72 to −0.85 V, and for $[Ru(\mathbf{5})_3]^{2+}$, the third ligand **5** is reduced at −0.97 V. The remaining auxiliary bpy ligands are reduced at potentials consistent with the parent $[Ru(bpy)_3]^{2+}$ complex and are shifted to slightly higher potentials due to the electronegativity of the bound **5**. The electrochemistry of the Os(II) complex is similar, with potentials spanning a slightly wider range (−0.51 to −1.07 V), reflecting the wider range of the MLCT absorption.

The aforementioned results are typical for heteroleptic Ru(II) complexes.[12] It is well established that in heteroleptic complexes possessing bpy, substituted bpy, and related ligands the photoexcited electron is localized on the ligand that is most easily reduced in the MLCT state.[12] Therefore, it is expected that the lowest-energy MLCT state in the $[Ru(bpy)_n(\mathbf{5})_{3-n}]^{2+}$ ($n = 0-2$) complexes is Ru → **5** in nature. The poor emission of the heteroleptic complexes can be

(11) (a) Breu, J.; Stoll, A. J. *Acta Crystallogr., Sect. C* **1996**, *52*, 1174−1177. (b) Maloney, D. J.; Macdonnell, F. M. *Acta Crystallogr., Sect. C* **1997**, *53*, 705−707. (c) Otsuka, T.; Sekine, A.; Fujigasaki, N.; Ohashi, Y.; Kaizu, Y. *Inorg. Chem.* **2001**, *40*, 3406−3412.

(12) (a) Yabe, T.; Orman, L. K.; Anderson, D. R.; Yu, S.-C.; Xu, X.; Hopkins, J. B. *J. Phys. Chem.* **1990**, *94*, 7128. (b) McClanahan, S. F.; Dallinger, R. F.; Holler, F. J.; Kincaid, J. R. *J. Am. Chem. Soc.* **1985**, *107*, 4853. (c) Danzer, G. D.; Kincaid, J. R. *J. Phys. Chem.* **1990**, *94*, 3976.

Table 2. Electrochemical Data for **5** and Complexes[a]

compound	$E_{1/2}$(ox)	$E_{1/2}$(red)
5	+1.40 (140)	−1.26 (100)
$[Ru(\mathbf{5})_3]^{2+}$	+1.27 (90)	−0.59 (70), −0.72 (100), −0.97 (80), −1.38 (60), −1.65 (110)
$[Ru(\mathbf{5})_2(bpy)]^{2+}$	+1.27 (80)	−0.67 (70), −0.85 (80), −1.36 (70), −1.57 (100)
$[Ru(\mathbf{5})(bpy)_2]^{2+}$	+1.27 (100)	−0.71 (80), −1.28 (100), −1.64 (100)
$[Ru(bpy)_3]^{2+}$[b]	+1.29	−1.33, −1.52, −1.76
$[Os(\mathbf{5})_3]^{2+}$	+0.93 (70)	−0.51 (70), −0.66 (80), −1.07 (130), −1.41 (70), −1.77 (100)

[a] Measured in CH_3CN at 25 °C, and potentials are reported in volts vs SCE. Most waves were reversible or quasi-reversible. The difference between anodic and cathodic waves is given in parentheses (mV). [b] From ref 1b.

understood in terms of recent experiments and calculations on related Ru(II) complexes with ligands possessing extended π-systems, such as dppz (dipyrido[3,2-a:2′,3′-c]phenazine). The introduction of π-extended ligands into the coordination sphere of heteroleptic Ru(II) complexes, such as in $[Ru(bpy)_2(dppz)]^{2+}$, results in an emissive MLCT state in equilibrium with a dark state, which lies just below the MLCT state.[13,14] Although the dark state was initially proposed to be a second MLCT state, calculations predict it to be a $^3\pi\pi^*$ state centered on the π-extended ligand.[14] Given the low energy of $^1\pi-\pi^*$ absorption of **5** (400−500 nm), a low-lying dark $^3\pi\pi^*$ state is not unlikely for the complexes possessing **5**. Although some of the reported complexes are emissive under certain conditions, the relative energies of the dark and emissive states, along with various rate constants, dictate whether luminescence is observed.[13] The poor emissive character of these complexes somewhat limits their utility as potential photoredox catalysts. However, the larger surface area of the ligand as compared to that of phen results in more oriented facets for its octahedral complexes which could engender interesting properties associated with intermolecular interactions used to probe shape specific biomolecules such as DNA.

DNA Binding and Photocleavage. Changes in the electronic absorption spectra of 3−5 μM **5** and $[Ru(\mathbf{5})_{3-n}(bpy)_n]^{2+}$ (n = 0, 1, 2) complexes (5 mM Tris buffer, pH = 7.5, 50 mM NaCl) were measured as a function of DNA concentration, and the titration curve for $[Ru(\mathbf{5})_2(bpy)]^{2+}$ is shown in Figure 3. In all cases, hypochromic or bathochromic shifts of $\pi\pi^*$ transitions of **5** and MLCT transitions of the Ru(II) complexes are observed, consistent with intercalation of **5** in the complex between the DNA bases.[15−17] For each compound, the hypochromicity and red shift associated with the peak at 441−447 nm are listed in Table 3. The observed values are typical of cationic metal complex intercalators, such as Ru(II) and Os(II) complexes possessing a dppz ligand.[15,16] The absorption change of a given compound with total concentration C_t is given by eq 1, where ϵ_f and ϵ_b represent the molar extinction coefficient of the free compound in solution and of that bound to DNA, respectively, and $\epsilon_a = A/C_t$, where A represents the absorption of the solution at a given DNA concentration.[16] Fits of plots of $(\epsilon_a - \epsilon_f)/(\epsilon_b - \epsilon_f)$ as a function of total DNA concentration, $[DNA]_t$, can be used to obtain the DNA binding constant, K_b, and binding site size, s, of the compound, which are listed in Table 3 and shown in Figure 4 for the free DAP ligand, $[Ru(bpy)_2(\mathbf{5})]^{2+}$, and $[Ru(\mathbf{5})_2(bpy)]^{2+}$.[16,18,19]

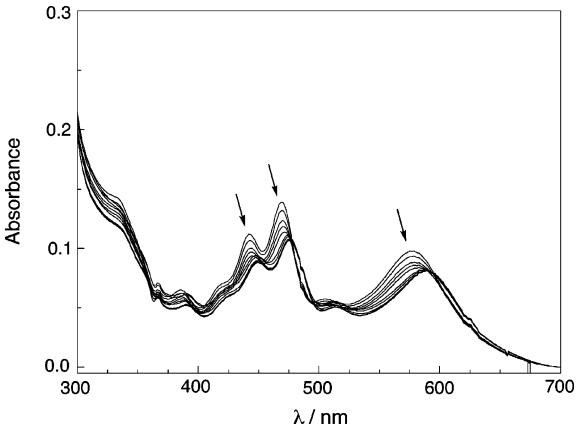

Figure 3. Changes in the electronic absorption spectrum of 4.0 μM $[Ru(\mathbf{5})_2(bpy)]^{2+}$ in 5 mM Tris buffer, pH = 7.5, 50 mM NaCl upon addition of 0, 2, 4, 6, 8, 14, 18, 22, 28, 34, 40, 50, and 60 μM calf-thymus DNA.

Table 3. Percent Hypochromicity, Bathochromic Shift, and Binding Constant, K_b, with s-Values from Fits of eq 1 at 441−447 nm

compound	% hypochromicity	shift (nm)	K_b (M^{-1})	s
5	27	7	2.7×10^5	0.4
$[Ru(bpy)_2(\mathbf{5})]^{2+}$	26	6	1.4×10^6	0.8
$[Ru(\mathbf{5})_2(bpy)]^{2+}$	20	8	1.6×10^6	1.4
$[Ru(\mathbf{5})_3]^{2+}$	14	6	*a*	*a*

$$\frac{(\epsilon_a - \epsilon_f)}{(\epsilon_b - \epsilon_f)} = \frac{b - (b^2 - 2K_b{}^2C_t[DNA]_t/s)^{1/2}}{2K_bC_t} \qquad (1)$$

$$b = 1 + K_bC_t + K_b[DNA]_t/2s$$

Unlike those of $[Ru(bpy)_2(\mathbf{5})]^{2+}$ and $[Ru(\mathbf{5})_2(bpy)]^{2+}$, the DNA titration of $[Ru(\mathbf{5})_3]^{2+}$ results in an initial hypochromic and bathochromic shift, followed by an increase in absorption at greater DNA concentrations; therefore, the absorption changes of $[Ru(\mathbf{5})_3]^{2+}$ were not fit to eq 1. The binding constants obtained for $[Ru(bpy)_2(\mathbf{5})]^{2+}$ and $[Ru(\mathbf{5})_2(bpy)]^{2+}$

(13) Brennaman, M. K.; Alstrum-Acevedo, J. H.; Fleming, C. N.; Jang, P.; Meyer, T. J.; Papanikolas, J. M. *J. Am. Chem. Soc.* **2002**, *124*, 15094.
(14) Pourtois, G.; Belijonne, D.; Moucheron, C.; Schumm, S.; Kirsh-De Mesmaeker, A.; Lazzaroni, R.; Brédas, J.-L. *J. Am. Chem. Soc.* **2004**, *126*, 683.
(15) (a) Holmlin, R. E.; Yao, J. A.; Barton, J. K. *Inorg. Chem.* **1999**, *38*, 174−189. (b) Holmlin, R. E.; Stemp, E. D. A.; Barton, J. K. *J. Am. Chem. Soc.* **1996**, *118*, 5236−5244.
(16) Nair, R. B.; Teng, E. S.; Kirkland, S. L.; Murphy, C. J. *Inorg. Chem.* **1998**, *37*, 139−141.
(17) Bradley, P. M.; Angeles-Boza, A. M.; Dunbar, K. R.; Turro, C. *Inorg. Chem.* **2004**, *43*, 2450−2452.
(18) Smith, S. R.; Neyhart, G. A.; Karlsbeck, W. A.; Thorp, H. H. *New J. Chem.* **1994**, *18*, 397−406.
(19) Carter, M. T.; Rodriguez, M.; Bard, A. J. *J. Am. Chem. Soc.* **1989**, *111*, 8901−8911.

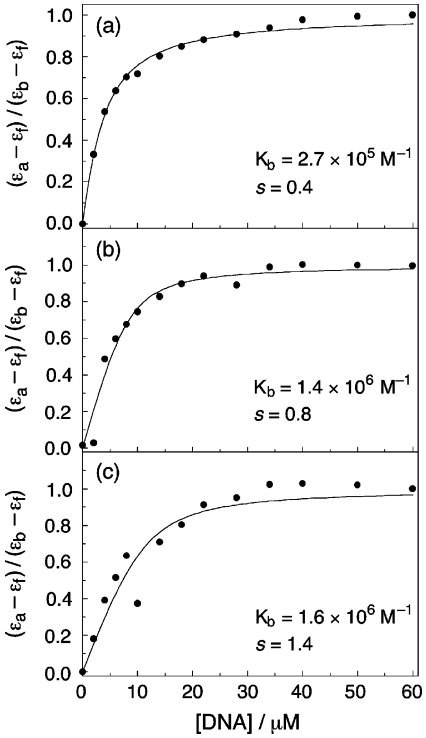

Figure 4. Fits to eq 1 of the optical changes upon addition of DNA to (a) 3.0 μM DAP ligand, (b) 4.9 μM $[Ru(bpy)_2(\mathbf{5})]^{2+}$, and (c) 4.0 μM $[Ru(\mathbf{5})_2(bpy)]^{2+}$ in 5 mM Tris buffer, pH = 7.5, 50 mM NaCl.

are similar in magnitude to those reported for other cationic metal complexes with intercalating ligands. Similar hypochromicity was reported for $[Ru(NH_3)_4(dppz)]^{2+}$ and $[Ru(phen)_2(dppz)]^{2+}$, which have been shown to bind to DNA through intercalation of the dppz ligand with binding constants, K_b, of 1.24×10^5 ($s = 0.02$) and $5.1 \times 10^6\ M^{-1}$ ($s = 0.6$), respectively.[16]

Because of the low solubility of the $[Ru(\mathbf{5})_2(bpy)]^{2+}$ and $[Ru(\mathbf{5})_3]^{2+}$ complexes in water and the higher complex concentrations required for viscosity and thermal denaturation experiments normally utilized for further confirmation of intercalation, these measurements were conducted only for $[Ru(bpy)_2(\mathbf{5})]^{2+}$. Intercalators have been known to shift the DNA melting temperature, T_m, to higher temperatures. The T_m values measured for 50 μM calf-thymus DNA in the presence and absence of 5 μM $[Ru(bpy)_2(\mathbf{5})]^{2+}$ in 1 mM phosphate buffer, pH = 7.5, and 2 mM NaCl were 58 ± 1 and 64 ± 1 °C, respectively. A ΔT_m of +5 °C was previously reported for the intercalator ethidium bromide ($K_b = 1.7 \times 10^5\ M^{-1}$).[20−22] The changes in the relative viscosity of solutions containing 200 μM sonicated herring sperm DNA upon addition of increasing concentrations of $[Ru(bpy)_2(\mathbf{5})]^{2+}$ are shown in Figure 5 and parallel those observed for ethidium bromide.[20,21] In contrast, addition of the minor groove binder Hoechst 33258 does not result in significant changes in the relative viscosity, which is typical for minor groove and electrostatic binders that do not intercalate

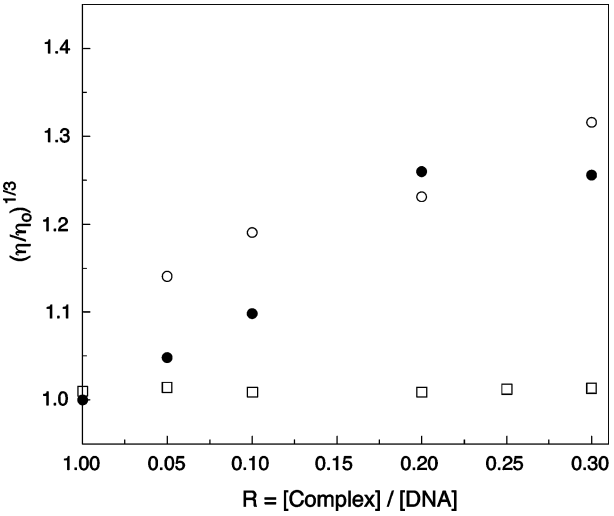

Figure 5. Changes in the relative viscosity of solutions containing 200 μM sonicated herring sperm DNA (5 mM Tris, pH = 7.5, 50 mM NaCl) as a function of the concentration of (○) ethidium bromide, (●) $[Ru(bpy)_2(\mathbf{5})]^{2+}$, and (□) Hoechst 33258.

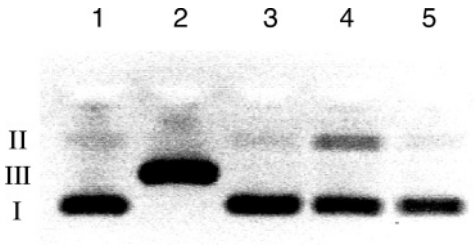

Figure 6. Ethidium bromide-imaged agarose gel (2%) of 100 μM pUC18 plasmid (5 μM Tris buffer, pH = 7.5, 50 μM NaCl) alone in the dark (lane 1), treated with *Sma*I (lane 2), and in the presence of 20 μM $[Ru(bpy)_2(\mathbf{5})]^{2+}$ in the dark (lane 3), irradiated (λ_{irr} > 395 nm, 30 min) in air (lane 4), and under N_2 (lane 5).

between the DNA bases.[23] Changes in relative viscosity provide a reliable method for the assignment of DNA binding modes by intercalators and groove binders. The viscosity data, taken together with the hypochromic shift of $[Ru(bpy)_2(\mathbf{5})]^{2+}$ upon addition of DNA and the shift in the DNA melting temperature, are in accord with an intercalative binding mode by the complex.

$[Ru(bpy)_2(\mathbf{5})]^{2+}$ is able to photocleave plasmid DNA upon irradiation with visible light in air. Figure 6 shows 100 μM pUC18 supercoiled plasmid DNA (form I) with some nicked, circular, impurities (form II) in lane 1 and that linearized by the reaction with *Sma*I (form III) in lane 2. The presence of 20 μM $[Ru(bpy)_2(\mathbf{5})]^{2+}$ in the dark does not result in DNA cleavage (lane 3); however, lane 4 shows the photocleavage of 100 μM pUC18 plasmid by 20 μM $[Ru(bpy)_2(\mathbf{5})]^{2+}$ (λ_{irr} > 395 nm, 30 min) in air with an increase in nick plasmid (form II). In contrast, irradiation under similar conditions and complex concentration under an N_2 atmosphere do not result in DNA cleavage (lane 5). These results are similar to those observed for other Ru(II) complexes, such as $[Ru(bpy)_3]^{2+}$ and $[Ru(phen)_3]^{2+}$, for which a reactive oxygen species, likely $^1O_2$, is believed to be responsible for the

(20) Tang, T.-C.; Huang, H.-J. *Electroanalysis* **1999**, *11*, 1185−1190.
(21) Paoletti, C.; Le Pecq, J. B.; Lehman, I. R. *J. Mol. Biol.* **1971**, *55*, 75−100.
(22) Fu, P. K.-L.; Bradley, P. M.; Turro, C. *Inorg. Chem.* **2003**, *42*, 878−884.
(23) (a) Suh, D.; Oh, Y.-K.; Chaires, J. B. *Process Biochem.* **2001**, *37*, 521−525. (b) Haq, I.; Lincoln, P.; Suh, D.; Norden, B.; Chowdhry, B. Z.; Chaires, J. B. *J. Am. Chem. Soc.* **1995**, *117*, 4788−4796.

observed DNA photocleavage.[24,25] The fact that the observed photocleavage in air is significantly lower than what is typically observed for $[Ru(bpy)_3]^{2+}$ possibly indicates lower levels of $^1O_2$ generation due to the shorter lifetime of the MLCT excited states of the complexes possessing **5** as ligands. To further support the involvement of $^1O_2$, the photocleavage was examined in D_2O (Supporting Information Figure S2). The increased photocleavage observed in D_2O (lane 4) relative to H_2O (lane 3) is indicative of a mechanism that involves the participation of $^1O_2$.

Experimental Section

Instrumentation. The microwave reactions were carried out in a household microwave oven modified according to a previously published description.[26] Nuclear magnetic resonance spectra were recorded at 300 MHz for ^1H and at 75 MHz for ^{13}C, referenced to TMS in $CDCl_3$ and to the solvent peak in all other solvents (CD_3CN). Electronic spectra were obtained on a Perkin-Elmer Lambda 3B spectrophotometer. Fluorescence spectra were obtained on a Perkin-Elmer LS-50 luminescence spectrometer. Cyclic voltammetry (CV) measurements were carried out in a conventional three-electrode cell with a BAS-27 voltammeter and a Houston Instruments model 100 X-Y recorder according to a previously described procedure.[27] Mass spectra were recorded on a Finnigan MAT model SSQ 700 quadrupole mass spectrometer fitted with an electrospray ionization source. The electrospray voltage was −3.5 kV. Samples were introduced by direct infusion of a solution at a concentration of about 5×10^{-11} mol/L at a flow rate of 1 μL/min. Elemental analyses were performed by QTI, P.O. Box 470, Whitehouse, NJ 08888-0470. Melting points were measured on a Hoover capillary melting point apparatus and are not corrected.

For DNA studies, absorption measurements were performed on a Hewlett-Packard diode array spectrophotometer (HP 8453) equipped with an HP 89090A temperature controller and HP 8453 Win System software. The source of visible radiation for the DNA photocleavage studies was the output of a 150 W Xe arc lamp with appropriate colored glass (high pass), filters (Oriel), and a 10-cm water cell (for removal of infrared light) positioned in the light path. The ethidium bromide-stained agarose gels used to determine the DNA photocleavage were imaged using a GelDoc 2000 transilluminator (Bio-Rad), and the ratio of the supercoiled, nicked (circular), and cut (linear) DNA was calculated using the intensity integration available in the Quantity One Analysis System (Bio-Rad) software. Viscosity measurements were carried out using 200 μM herring sperm DNA on a Cannon-Manning Micro viscometer immersed in a water bath maintained at 25 °C with a Neslab RTE-100 circulating temperature control unit. The flow time was recorded using a digital stopwatch, and each sample was measured three times and an average flow time calculated. Relative viscosity for DNA in either the presence or absence of metal complexes and metal ions was calculated using standard methods.[23]

Materials. The *cis*-$[Ru(bpy)_2Cl_2]$,[28] $Ru(DMSO)_4Cl_2$,[29] and 1,1′-biisoquinoline[30] starting materials were prepared according to known procedures. Agarose and ethidium bromide were purchased from Aldrich and used without further purification. The pUC18 plasmid was purchased from New England Biolabs and purified using a rapid plasmid miniprep system (Marligen Bioscience). Calf-thymus DNA was purchased from Sigma and was purified by reported methods.[31] DNA loading solution (5×, 0.25% w/v bromophenol blue, 0.25% w/v xylene cyanole FF, 40% w/v sucrose, pH = 8) and TAE (10×, 0.4 M Tris acetate, 10 mM EDTA, pH = ∼8.2) buffer were purchased from Sigma and used as received. The *Sma*I restriction enzyme was purchased from Invitrogen Life Technology. CH_3CN, used for cyclic voltammetry, was dried by reflux with calcium hydride followed by distillation. All other solvents were used without further purification.

1,12-Diazaperylene (5, DAP).[8] In a round-bottomed flask under a stream of Ar, 1,1′-biisoquinoline (0.5 g, 1.95 mmol) was dissolved in dry 1,2-dimethoxyethane (8 mL). Potassium (1.29 g, 33.1 mmol), which was separated from its oxide layer and shredded into small pieces, was then added. The intensely colored blue mixture was stirred at room temperature for 16 h, after which time the remaining potassium was removed under Ar, and the solution was stirred under a stream of dry air for an additional 4 h. The solvent was evaporated, and the residue was chromatographed on basic Al_2O_3, eluting with CH_2Cl_2/hexane to give **5** (120 mg, 24%) as a yellow solid (mp > 270 °C). ^1H NMR ($CDCl_3$): δ 8.82 (d, 1H, H_2, J = 6.0 Hz), 8.32 (dd, 1H, H_6, J = 7.5, 1.5 Hz), 7.43 (m, 2H, $H_{4,5}$), 7.65 (d, 1H, H_3, J = 6.0 Hz). ^{13}C NMR ($CDCl_3$): δ 151.0, 147.2, 145.1, 137.3, 130.9, 127.7, 125.2, 122.5, 122.0. MS: *m*/*z* 254 (100%, (M + 1)).

***cis*-$[Ru(5)_2Cl_2]$.** $RuCl_3 \cdot 3H_2O$ (20.5 mg, 0.08 mmol), 1,12-diazaperylene (**5**, 40 mg, 0.16 mmol), and LiCl (22.0 mg, 0.52 mmol) in DMF (5 mL) were refluxed for 8 h under Ar. After cooling the mixture, we added acetone (2 mL), and the mixture was cooled to 0 °C. Filtration yielded a violet solution and a dark black solid. The solid was washed with H_2O (3 × 1 mL) followed by diethyl ether (2 × 1 mL) and then dried to afford a dark purple material (30 mg, 52%) which was used without further purification.

$[Ru(5)_2(bpy)](PF_6)_2$. A mixture of bpy (6.53 mg, 0.04 mmol) and *cis*-$[Ru(5)_2Cl_2]$ (30.0 mg, 0.04 mmol) in ethylene glycol (5 mL) was heated in a microwave oven under Ar for 30 min at 5 min intervals. After cooling the mixture, we poured it into H_2O (20 mL). Excess NH_4PF_6(aq) (49 mg, 0.3 mmol) was added, and the mixture was stirred for 15 min. The precipitate was filtered, dried, dissolved in a minimum amount of CH_3CN, and purified by chromatography on basic Al_2O_3, eluting with toluene/CH_3CN (7:3) to provide a green solid (20 mg, 46%) (mp > 280 °C). ^1H NMR (CD_3CN): δ 8.77 (dd, 1H, J = 7.0, 1.3 Hz), 8.72 (d, 1H, J = 5.2 Hz), 8.53 (d, 1H, J = 8.1 Hz), 8.14 (d, 1H, J = 7.8 Hz), 8.08 (d, 1H, J = 7.8 Hz), 8.02−7.99 (m, 3H), 7.95 (d, 1H, J = 5.7 Hz), 7.80 (d, 1H, J = 6.5 Hz), 7.74 (d, 1H, J = 5.7 Hz), 7.65 (d, 1H, J = 5.4 Hz), 7.35 (dd, 1H, J = 7.0, 1.3 Hz). MS: *m*/*z* 766 (100%, (M + 1) − $2PF_6$). Anal. Calcd for $C_{46}H_{28}N_6RuP_2F_{12} \cdot H_2O$: C, 51.44; H, 2.80; N, 7.83. Found: C, 51.77; H, 3.20; N, 6.52.

$[Ru(5)(bpy)_2](PF_6)_2$. A mixture of **5** (53.3 mg, 0.21 mmol) and *cis*-$[Ru(bpy)_2Cl_2]$ (119 mg, 0.23 mmol) in ethylene glycol (5 mL) was heated in a microwave oven under Ar for 30 min at 5 min intervals. After cooling the mixture, we poured it into H_2O (20 mL). Excess NH_4PF_6(aq) (49 mg, 0.3 mmol) was added, and the mixture was stirred for 15 min. The precipitate was filtered, dried,

(24) Fu, P. K.-L.; Bradley, P. M.; van Loyen, D.; Dürr, H.; Bossmann, S. H.; Turro, C. *Inorg. Chem.* **2002**, *41*, 3808−3810.
(25) Hergueta-Bravo, A.; Jimenez-Hernandez, M. E.; Montero, F.; Oliveros, E.; Orellana, G. *J. Phys. Chem. B* **2002**, *106*, 4010−4017.
(26) (a) Matsumura-Inoue, T.; Tanabe, M.; Minami, T.; Ohashi, T. *Chem. Lett.* **1994**, 2443. (b) Arai, T.; Matsumura, T.; Oka, T. *Kagaku to Kyoiku* **1993**, *41*, 278.
(27) Goulle, V.; Thummel, R. P. *Inorg. Chem.* **1990**, *29*, 1767.
(28) Sullivan, B. P.; Salmon, D. J.; Meyer, T. J. *Inorg. Chem.* **1978**, *17*, 3334.
(29) Evans, I. P.; Spencer, A.; Wilkinson, G. *J. Chem. Soc., Dalton Trans.* **1973**, 204.
(30) Ashby, M. T.; Govindan, G. N.; Grafton, A. K. *J. Am. Chem. Soc.* **1994**, *116*, 4801.
(31) Sambrook, J.; Russel, D. W. *Molecular Cloning, a Laboratory Manual*; Cold Spring Harbor: New York, 2001.

dissolved in a minimum amount of CH_3CN, and purified by chromatography on basic Al_2O_3, eluting with toluene/CH_3CN (7:3) to provide a green solid (136 mg, 68%) (mp > 280 °C). ^{1}H NMR (CD_3CN): δ 8.74 (d, 1H, H_6, J = 7.7 Hz), 8.53 (d, 1H, H_{3a}, J = 8.5 Hz), 8.46 (d, 1H, H_{3b}, J = 8.5 Hz), 8.15−7.96 (m, 4H), 7.86 (d, 1H, H_3, J = 6.0 Hz), 7.81 (d, 1H, H_{6a}, J = 5.4 Hz), 7.67 (d, 1H, H_2, J = 6.0 Hz), 7.65 (d, 1H, H_{6b}, J = 5.4 Hz), 7.45 (t, 1H, H_{5a}, J = 7.1 Hz), 7.22 (t, 1H, H_{5b}, J = 7.1 Hz). MS: m/z 511 (100%, (M − 2PF_6 − bpy)). Anal. Calcd for $C_{38}H_{26}N_6RuP_2F_{12}\cdot H_2O$: C, 46.77; H, 2.87; N, 8.62. Found: C, 47.13; H, 2.37; N, 8.06.

[Ru(5)$_3$](PF$_6$)$_2$. A mixture of 1,12-diazaperylene (**5**, 91 mg, 0.36 mmol) and $RuCl_3\cdot 3H_2O$ (24 mg, 0.092 mmol) in ethylene glycol (8 mL) was heated in a microwave oven for 10 min. After cooling the mixture, we poured it into H_2O (60 mL). Excess NH_4PF_6 (163 mg, 1.0 mmol) was added, and the mixture was stirred for 30 min. The precipitate was filtered, dried, and purified by chromatography on basic Al_2O_3, eluting with CH_2Cl_2/CH_3CN (3:1) to provide a black solid (75 mg, 71%) (mp > 280 °C). ^{1}H NMR (CD_3CN): δ 8.75 (dd, 2H, H_6, J = 7.2, 1.2 Hz), 8.05 (m, 4H, $H_{4,5}$), 7.85 (d, 2H, H_3, J = 6.3 Hz), 7.78 (d, 2H, H_2, J = 6.3 Hz). ^{13}C NMR (CD_3CN): δ 156.1, 146.0, 137.0, 134.2, 130.8, 129.1, 127.4, 126.7, 126.5. MS: m/z 863 (100%, (M − 2PF_6)). Anal. Calcd for $C_{54}H_{30}N_6RuP_2F_{12}\cdot H_2O$: C, 55.33; H, 2.73; N, 7.17. Found: C, 54.93; H, 2.80; N, 7.10.

[Os(5)$_3$](PF$_6$)$_2$. A mixture of 1,12-diazaperylene (**5**, 50 mg, 0.2 mmol) and [K_2OsCl_6] (31.6 mg, 0.066 mmol) in ethylene glycol (10 mL) was refluxed for 6 h under Ar. After cooling the mixture, we added excess NH_4PF_6(aq), and the mixture was stirred for 15 min. The green precipitate was filtered, dried, dissolved in a minimum amount of CH_2Cl_2, and chromatographed on basic Al_2O_3, eluting with CH_2Cl_2/MeOH (99:1). The second fraction gave a green solid (20 mg, 24%) (mp > 280 °C). ^{1}H NMR (CD_3CN): δ 8.69 (d, 1H, H_6, J = 7.4 Hz), 8.04 (m, 2H, $H_{4,5}$), 7.76 (d, 1H, H_3, J = 6.3 Hz), 7.69 (d, 1H, H_2, J = 6.2 Hz). MS: m/z 953 (100%, (M + 1) − 2PF_6).

Methods. DNA Photocleavage in Vitro. The DNA photocleavage was carried out on a 20 μL total sample volume in 0.5 mL transparent Eppendorf microtubes containing 100 μM pUC18 plasmid. Irradiation of the reaction mixtures was conducted either in air or under a positive pressure of nitrogen atmosphere following bubbling for ∼15 min. DNA gel loading solution (4 μL, resulting in 0.042% w/v bromophenol blue, 0.042% w/v xylene cyanole FF, and 6.7% w/v sucrose) was added to each reaction mixture, and the electrophoresis was carried out using a 2% agarose gel stained with 0.5 mg/L ethidium bromide in 1× TAE running buffer (40 mM Tris acetate, 1 mM EDTA, pH = ∼8.2) at 65 V for 2 h. These conditions were chosen to efficiently separate the imaged nicked (circular, form II) and cut (linear, form III) forms of the plasmid.

X-ray Structure Determination. Data were collected at 110 K on a Bruker GADDS diffractometer equipped with a multiwire 2D area detector and graphite monochromated Cu Kα radiation (α = 1.5418 Å). The program FRAMBO[32] was used to collect the data (Table 4).

The data were collected using 0.5° ω-scans in the θ range of 2.45 to 49.61° with a detector-to-crystal distance of 6 cm. The reflections were indexed using a C-centered monoclinic cell. The diffraction intensities were integrated with the SAINT software package[33] and corrected for absorption using SADABS.[34] The space group $C2/c$ was chosen on the basis of the systematic absences in the diffraction patterns and the intensity statistics. The structure was solved and refined using X-SEED,[35] a graphical interface to SHELX97.[36] In this structure, the asymmetric unit contains two ordered mononuclear [$Ru^{II}(L)_3$] residues which appear to be chemically equivalent but not crystallographically equivalent. All non-hydrogen atoms of both [$Ru^{II}(L)_2$)]$_3$ units and atoms belonging to a disordered [PF_6]$^-$ anion were located from the Fourier maps. The remaining residual electron density was extremely diffuse with only three peaks larger than 2 e Å^{-3} corresponding to disordered solvent and counterions located in a large region of the unit cell. It was difficult to assign atoms in this region with certainty. The electron density in this area (including disordered [PF_6]$^-$ anions) was accounted for by the SQUEEZE program[37] of PLATON.[38] This program modifies the observed structure factors by subtracting the contributions to them from the electron density in the disordered region. This region occupies a total of 8847 Å^{-3} per unit cell, and the electron density removed by the *SQUEEZE* procedure amounts to 4193 electrons per unit cell. In the final cycles of refinement, all of the non-hydrogen atoms were refined anisotropically. The hydrogen atoms were refined in a riding mode with values of U_{eq} that were 1.2 times that of the U_{eq} for the C atoms to which they were bonded. The final refinement was based on 76 611 reflections, of which 10 678 reflections were unique (3985 greater than 2σ), 1111 parameters, and 2205 restraints. Refinement converged at R1

Table 4. Data Collection and Processing Parameters for [Ru(DAP)$_3$](PF$_6$)$_2$

empirical formula	$C_{54}H_{30}N_6Ru$
fw	863.91
temp	110(2) K
wavelength	1.54180 Å
cryst syst	monoclinic
space group	$C2/c$
unit cell dimensions	a = 48.04(3) Å b = 12.707(8) Å c = 37.56(2) Å α = 90° β = 106.016(19)° γ = 90°
vol	22040(25) Å^3
Z	16
density (calcd)	1.041 Mg/m^3
abs coeff	2.571 mm^{-1}
F(000)	7040
cryst size	0.37 × 0.28 × 0.09 mm^3
θ-range for data collection	2.45−49.61°
index ranges	$-47 \le h \le 47$, $-12 \le k \le 12$, $-36 \le l \le 36$
reflns collected	76611
independent reflns	10678 [R(int) = 0.1506]
completeness to θ = 49.61°	95.9%
abs correction	semiempirical from equivalents
max and min transmission	0.8016 and 0.4497
refinement method	full-matrix least-squares on F^2
data/restraints/params	10678/2205/1111
GOF on F^2	0.739
final R indices [$I > 2\sigma(I)$]	R1 = 0.0472, wR2 = 0.0867
R indices (all data)	R1 = 0.1367, wR2 = 0.0992
largest diff. peak and hole	0.187 and −0.416 e Å^{-3}

(32) *FRAMBO*, version 41.33; program for data collection on area detectors; Bruker AXS, Inc.: Madison, WI, 2003.

(33) *SAINT*, version 6.34; Bruker AXS, Inc.: Madison, WI, 2001.
(34) Barbour, L. J. *Supramol. Chem.* **2001**, *1*, 189−191.
(35) *SADABS*; Bruker AXS, Inc.: Madison, WI, 2003.
(36) Sheldrick, G. M. *SHELX*: *Programs for Solving and Refining Crystal Structures*; University of Göttingen: Göttingen, Germany, 1997.
(37) van der Sluis, P.; Spek, A. L. *Acta Crystallogr., Sect. A* **1990**, *46*, 194−201.
(38) Spek, A. L. *J. Appl. Crystallogr.* **2003**, *36*, 7−13.

= 0.0472 and at a goodness-of-fit (GOF) value of 0.732. The highest residual peak is 0.187 e $Å^{-3}$, and the deepest hole is −0.416 e $Å^{-3}$.

Acknowledgment. R.P.T. and A.C. thank the Robert A. Welch Foundation (E−621) and the Division of Chemical Sciences, Office of Basic Energy Sciences, U.S. Department of Energy (Contract DE-FG03-02ER15334), for financial support of this work. C.T. thanks the National Institutes of Health (RO1 GM64040-01) for their generous support. K.R.D. gratefully acknowledges the National Science Foundation for funds to purchase the CCD X-ray diffractometer (NSF 9807975).

Supporting Information Available: X-ray crystallographic files for $[Ru(\mathbf{5})_3](PF_6)_2$ (in CIF format), an expanded view of the unit cell (Figure S1), and ethidium bromide stained agarose gel of pUC18 with $[Ru(bpy)_2(\mathbf{5})]^{2+}$ irradiated with $\lambda > 395$ nm (Figure S2). This material is available free of charge via the Internet at http://pubs.acs.org.

IC0485965